Available online at www.sciencedirect.com

SciVerse ScienceDirect

Ceramics International 38 (2012) 2313–2317

CERAMICS INTERNATIONAL

www.elsevier.com/locate/ceramint

The simple one-step solvothermal synthesis of nanostructurated $VO_2(B)$

Sanja Milošević [a], Ivana Stojković [b], Sandra Kurko [a], Jasmina Grbović Novaković [a], Nikola Cvjetićanin [b,*]

[a] *Department of Materials Science, Vinča Institute of Nuclear Sciences, 11000 Belgrade, Serbia*
[b] *Faculty of Physical Chemistry, University of Belgrade, 11158 Belgrade 118, Serbia*

Received 15 September 2011; received in revised form 31 October 2011; accepted 1 November 2011
Available online 6 November 2011

Abstract

$VO_2(B)$ has been successfully synthesized by simple, facile and environmental friendly one-step solvothermal method using V_2O_5 and ethanol as a starting agent. Obtained micrometer-sized powder was composed from mutually welded nanosized rod-like, flat and snowflake structures. $VO_2(B)$ powder was tested for possible application as anode material for aqueous lithium ion batteries. Lithium intercalation/deintercalation reaction has been carried out by cyclic voltammetry in a saturated aqueous solution of $LiNO_3$. At scan rate of 10 mV s^{-1} very stable cyclic performance of such obtained VO_2 was established with discharge capacity around 184 mAh g^{-1}.

Keywords: C. Electrical properties; D. Transition metal oxide; E. Batteries; Hydrothermal/solvothermal synthesis

1. Introduction

Among the transition metal oxides, vanadium dioxide (VO_2) with four different polymorphic structures appears to be a particularly attractive material for various important applications. As a result of a reversible first-order metal–insulator transition at a temperature of $T_c = \sim 68\ ^\circ C$ (340 K) [1–4] monoclinic vanadium dioxide $VO_2(M)$ has been considered for applications in field-effect transistors [5,6] switches [7–9] sensors [10,11] and smart windows [12,13]. On the other hand, metastable $VO_2(B)$ is a promising anode material for aqueous lithium ion batteries [14–16] due to a proper electrode potential and tunnel structure that enables reversible intercalation and deintercalation of lithium ions [17]. In the past fifteen years the interest in studies of Li^+ ion batteries with aqueous electrolytes has grown exponentially since aqueous electrolytes are cheap, environmental friendly and nontoxic [14–16,18–21].

The hydrothermal/solvothermal synthesis (HT/ST) is the most commonly reported method for synthesis of VO_2. The benefits of these methods are the relatively low required temperature, environmental friendly reaction conditions, and controllable morphology and size distribution. Table 1 shows a review of $VO_2(B)$ HT/ST synthesis routes according to the literature data together with our results.

It can be seen from Table 1 that HT/ST synthesis of $VO_2(B)$ and $VO_2(M)$ is delicate because it greatly depends on parameters such as temperature, time of synthesis and pH value [2,22]. The adjusting those parameters to get pure phase is usually an intricate task. $VO_2(B)$ exhibits different morphology: from nanowires and nanobelts to urchin and flower-like, depending on terms of synthesis. Different precursors lead to different post treatment of product. Starting temperatures are relatively high, while the time of synthesis goes from 12 to 48 h (see Table 1). On the other hand it is very difficult to obtain pure $VO_2(B)$ phase: Son et al. [2] reported a mixture of two polymorph phases $VO_2(B)$ and $VO_2(M)$ when HT synthesis was performed at 220 °C during 48 h.

All four VO_2 polymorphs, $VO_2(R)$, $VO_2(M)$, $VO_2(B)$, and $VO_2(A)$, are based on an oxygen bcc lattice, with vanadium in octahedral sites of the more or less regular oxygen octahedra. They can be separated into two groups, depending on the mutual orientation of the fourfold axis of the oxygen octahedra. The oxygen octahedra can be aligned either along two perpendicular directions, as in the case of $VO_2(R)$ (rutile structure) and $VO_2(M)$ (monoclinic deformed structure); or

---

* Corresponding author at: Faculty of Physical Chemistry, University of Belgrade, 11158 Belgrade 118, PAC 105305, Serbia.
Tel.: +381 11 3336623; fax: +381 11 2187133.
E-mail address: nikola.cvj@ffh.bg.ac.rs (N. Cvjetićanin).

0272-8842/$36.00 © 2011 Elsevier Ltd and Techna Group S.r.l. All rights reserved.
doi:10.1016/j.ceramint.2011.11.001

Table 1
HT/ST synthesis of $VO_2(B)$: literature data and our results.

Literature	Synthesis mode *T* (°C), *t* (h)	Precursor	Crystal structure and morphology
[17]	200, 24	$V(IV)O(acac)_2$ + PVP solution	Monoclinic $VO_2(B)$ ($C2/m$) SEM: flowerlike morphology
[22]	180, 24	NH_4VO_3 + deionized H_2O + HCOOH	Monoclinic $VO_2(B)$ ($C2/m$) SEM: nanobelts
[23]	180, 12	V_2O_5 + ethylene glycol + distilled H_2O	$VO_2(B)$ monoclinic ($C2/m$) TEM: nanowire arrays
[24]	180, 24	V_2O_5 + aqueous solution with different concentrations of oxalic acid	Monoclinic $VO_2(B)$ nanobelts, nanosheets and olive-like nanostructures
[25]	180, 24	V_2O_5 + glukcose (in molar ratio 1:1) + deionized H_2O	Monoclinic $VO_2(B)$ ($C2/m$) SEM: belt-like morphology
[26]	180, different reaction times 36, 48	V_2O_5 + PDDA polyelectrolyte	Monoclinic $VO_2(B)$ SEM: rod-like morphology
[27]	180, different reaction times 12, 24	V_2O_5 + H_2O_2 + distilled H_2O + oxalic acide	Monoclinic $VO_2(B)$ SEM: urchin-like morphology and nanosheets
[28]	180, 48	$V_2O_5{\cdot}nH_2O$ sols + $H_2C_2O_4{\cdot}2H_2O$	Monoclinic $VO_2(B)$ ($C2/m$) SEM: nanobelt morphology
Our results	160, 24	V_2O_5 + ethil alcohol	Monoclinic $VO_2(B)$ ($C2/m$) SEM: different nanounits welded in micrometer-sized structures

oxygen octahedra can be mainly aligned along one direction as in $VO_2(B)$ and $VO_2(A)$ [1]. Under HT conditions $VO_2(A)$ is the intermediate phase during transition from the metastable monoclinic $VO_2(B)$ to the stable tetragonal rutile $VO_2(R)$ phase. Based on theoretical investigation and in situ electron microscopy Leroux et al. gave the complete description of crystallographic structures of all four oxides [1].

Although there is waste literature data on HT/ST synthesis, one step solvothermal synthesis at low temperatures has not been achieved yet. For that reason in this paper we report a simple one step ST synthesis of pure $VO_2(B)$ starting from V_2O_5 and ethanol, without addition of any surfactants or any post thermal treatment. The structure and morphology of obtained powder material were characterized by X-ray powder diffraction (XRD) and scanning electron microscopy (SEM), respectively. Its possible application as cathode and anode material in rechargeable Li-ion batteries has been tested by cyclic voltammetry (CV). The CV is a fast and simple electrochemical method to test cathodic and anodic materials in aqueous solution, and to predict their long-term constant current cycling behavior [20,21].

2. Materials and methods

Nanostructurated $VO_2(B)$ has been synthesized by ST method using 32 ml teflon lined autoclave. 230 mg of vanadium pentoxide (Merck 99.99%) and 22.5 ml of ethanol (Merck 96%) were stirred vigorously (magnetic stirrer) for 30 min before filling autoclave. Reaction in autoclave occurred at $T = 160$ °C for 24 h. Autoclave was then allowed to gradually cool down to room temperature. The dark blue precipitate was rinsed several times with ethanol, centrifuged and then dried in the oven at $T = 50$ °C for 2 h. The mass of obtained powder was around 208 mg, which is close to theoretical value for complete conversion of V_2O_5 to VO_2.

The X-ray powder diffraction measurements were performed by Siemens Kristallflex D-500 diffractometer using Cu K$\alpha_{1,2}$ Ni filtrated radiation in $2\theta^\circ$ range from 10 to 75° using 0.02° step and exposition time of 5 s. The crystallite size was obtained by Cauchy/Gaussian approximation.

Morphological characterization was carried out by SEM VEGA TS 5130MM, Tescan Brno.

Cyclic voltammograms were recorded using Gamry PCI4/300 Potentiostat/Galvanostat. All CV experiments were conducted in a three-electrode cell with $VO_2(B)$ as a working electrode, a wide platinum foil as counter electrode, and a saturated calomel electrode (SCE) as the reference one. The working electrodes were prepared in the following way: 85 wt.% of the active powder, 10 wt.% of carbon black and 5 wt.% of poly(vinylidene fluoride) (PVDF) binder were added together to *N*-methyl-2-pyrrolidone solvent. This slurry was homogenized for 30 min in an ultrasonic bath, and one drop was taken and spread over a glassy carbon stick, which was then heated under vacuum at 140 °C for about 4 h in order to let the solvent evaporate. The saturated aqueous solution of $LiNO_3$ was used as electrolyte. The cyclovoltammograms were recorded at a scan rate of 10 mV s^{-1} in the potential range from +0.5 V to −1 V vs. SCE.

3. Results and discussion

The blue-black precipitate is obtained after ST synthesis indicating that the reduction from V^{5+} to V^{4+} occurred. The diffraction pattern shown in Fig. 1 can be entirely indexed to a pure monoclinic $VO_2(B)$ according to JCPDS Card No. 31-1438. Vertical bars are placed at the positions of Bragg reflections. The broad diffraction peaks indicate that the powder is nanocrystalline. In fact, calculated crystallite size from Cauchy/Gaussian approximation is around 15 nm. It is obvious that the use of ethanol as solvent and reducing agent enabled ST synthesis of pure crystalline $VO_2(B)$ powder at 160 °C without using surfactants and subsequent thermal treatment. According to our knowledge (see Table 1), 160 °C is the lowest ST synthesis temperature reported so far.

Fig. 2 shows SEM images of $VO_2(B)$ synthesized solvothermally. The product consists of a large amount of irregular flat particles, significant concentration of rods and the small amount of snowflake particles. The thickness of flat particles and rods is around 200 nm while the length of rods is under 5 μm (Fig. 2a). Single particles mostly less than 400 nm

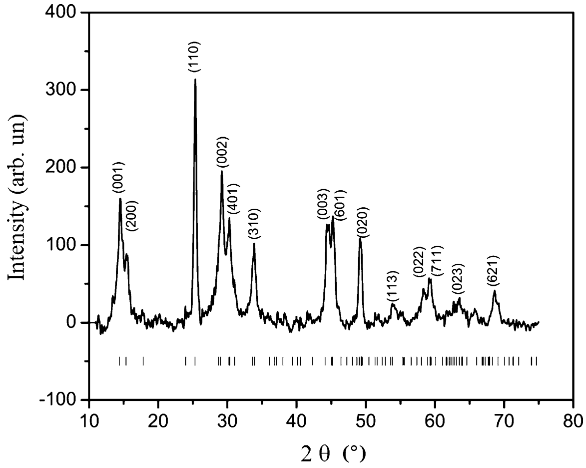

Fig. 1. XRD pattern of $VO_2(B)$ powder material obtained by ST synthesis. Vertical markers indicate the position of Bragg reflections of $VO_2(B)$ according to JCPDS Card No. 31-1438.

are melted together in different structures (Fig. 2a). Some amount of flower-like structures can be also observed (Fig. 2b and c). Generally, all nanounits are mutually welded in different micrometer-sized structures. Many pores with different diameter sizes can be also observed among the agglomerates. These pores may serve as transport paths for small molecules and ions, and also enhance contact area with nanosized particles (Fig. 2c). Cao et al. [29] reported similar results using a method of hydrothermal synthesis of W-doped VO_2 rutile-type powders by using V_2O_5 in oxalic acid blending with a small amount of tungstenic acid via one-step hydrothermal reactions at 240 °C.

Although the reason for formation of different nano-shapes of $VO_2(B)$ is still unclear, the existence of welded, i.e. strongly bonded particles most likely indicates dissolution–precipitation mechanism of ST reaction [30]. Ethanol has lower relative dielectric constant than water, but being more volatile than water it develops higher autogenerated pressure. Such pressure is probably the main driving force for ST reaction to occur at 160 °C in 96% ethanol. Small amount of water in the autoclave may contribute to the dissolution process of V_2O_5, but larger fraction would decrease the reducing power of ethanol [31].

The CV curves of ST obtained $VO_2(B)$, recorded at a scan rate of $10\ \mathrm{mV\ s^{-1}}$, are shown in Fig. 3. The voltammograms indicate preferably one stage intercalation/deintercalation process of Li^+ ions. The position of cathodic/anodic peak corresponding to Li^+ intercalation/deintercalation stands at −0.68 V/−0.46 V vs. SCE respectively. Both peaks are

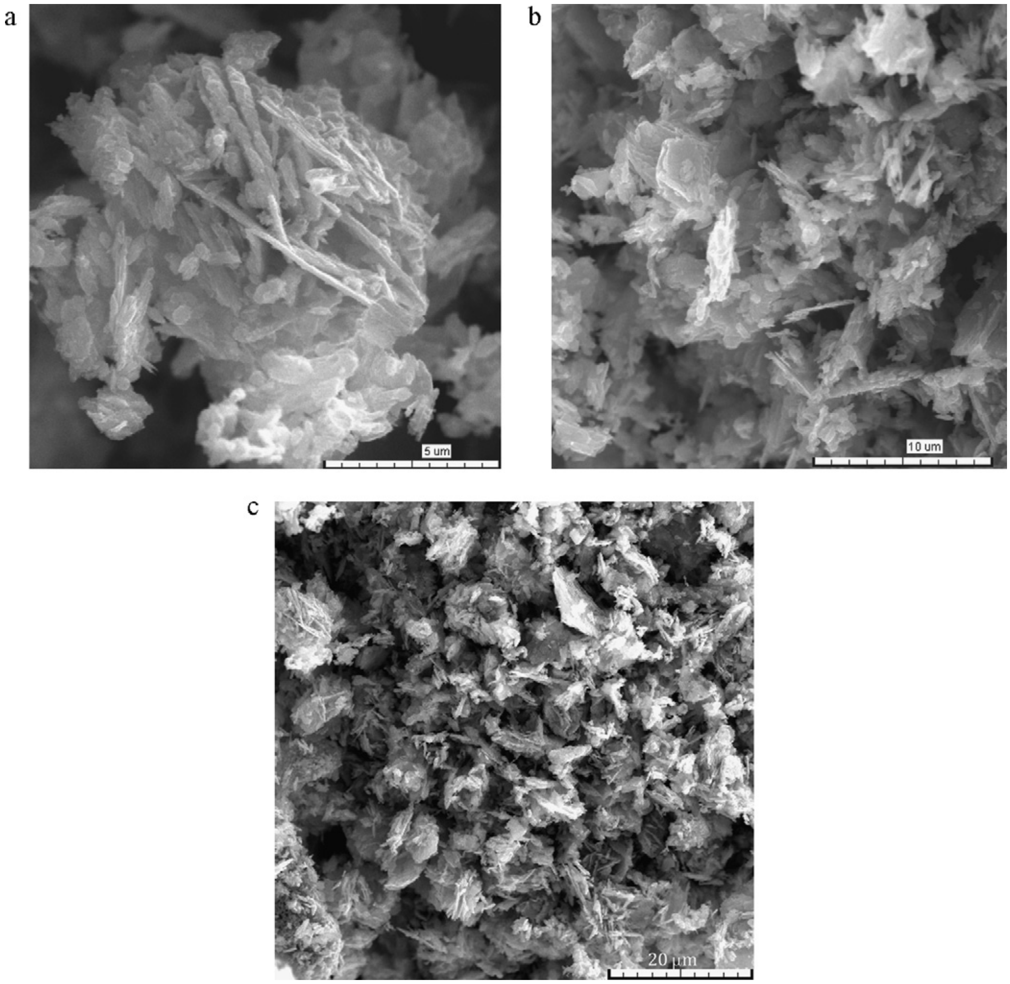

Fig. 2. SEM images of solvothermally synthesized $VO_2(B)$: (a) different nanounits welded in micrometer-sized structure, (b) snowflake- and flower-like structures and (c) the presence of void space between micrometer-sized particles.

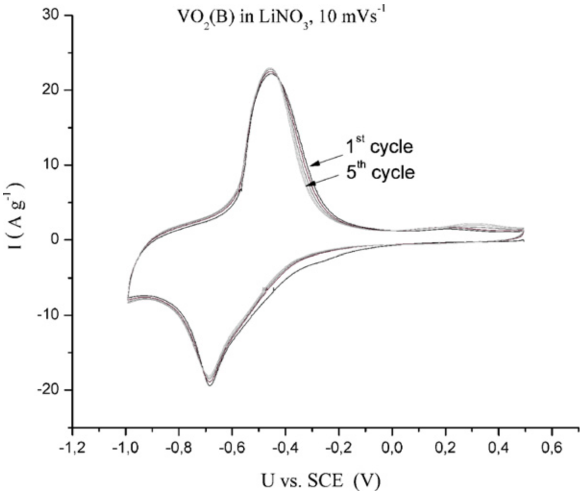

Fig. 3. Cyclic voltammograms of $VO_2(B)$ in saturated $LiNO_3$ aqueous solution, at a scan rate of 10 mV s^{-1}.

significantly shifted towards negative potentials comparing to values obtained for V_2O_5 xerogel [18,19]. A capacity fade is negligible in the next four cycles. The charge and discharge capacities calculated from cyclic voltammograms are similar and amount approximately 184 mAh g^{-1}. This capacity value is a significant one for this kind of electrode material in aqueous electrolyte, especially having in mind that sweep rate of 10 mV s^{-1} is very high for the lithium intercalation/deintercalation process [32]. Discharge capacity of nano-$VO_2(B)$ in organic electrolytes drops in the first few cycles and depends very much on the type of electrolyte and the size of nanostructures [33]. Self-assembling of nanounits into micrometer-scale structures seems to give robustness to $VO_2(B)$ so it can sustain electrochemical cycling without significant capacity drop [17,34]. The very good performance in CV experiments obtained here is most likely due to both micro-nano morphology and the use of water based electrolyte. We suppose that nanounits welded in microstructures exposed to highly conductive aqueous electrolyte are strong enough to enable fast insertion and extraction of lithium from a large surface area of material without or with very small changes in its structure. These properties of $VO_2(B)$, prepared here by simple ST method, make it a good candidate for anodic material for aqueous lithium battery. In combination with appropriate cathodic materials [20,21] it can be used for assembling the aqueous lithium battery which can deliver voltage over 1.5 V.

4. Conclusion

$VO_2(B)$ powder has been successfully synthesized through one-step solvothermal method starting from V_2O_5 and ethanol, without using surfactants and subsequent thermal treatment. The synthesized $VO_2(B)$ powder exists as a micrometer-sized structures obtained from welding of different nanounits. Appropriate electrode potential and stable cyclic performance with high capacity make this material a perspective anode material for aqueous lithium ion batteries with voltages even higher than 1.5 V. However, the performances should be additionally tested by long term galvanostatic experiments.

Acknowledgments

The work is financially supported by Serbian Ministry of Science and Technical Development under project III 45014 and III 45012. Authors want to express their gratitude to Zvezdana Baščarević for recording SEM micrographs.

References

[1] C. Leroux, G. Nihoul, G. Van Tendeloo, From $VO_2(B)$ to $VO_2(R)$: theoretical structures of VO_2 polymorphs and in situ electron microscopy, Phys. Rev. B 57 (1998) 5111–5121.
[2] J.H. Son, J. Wei, D. Cobden, G. Cao, Y. Xia, Hydrothermal synthesis of monoclinic VO_2 micro- and nanocrystals in one step and their use in Fabricating Inverse Opals, Chem. Mater. 22 (2010) 3043–3050.
[3] S.A. Corr, D.P. Shoemaker, B.C. Melot, R. Seshadri, Real-space investigation of structural changes at the metal–insulator transition in VO_2, Phys. Rev. Lett. 105 (2010) 056401–056404.
[4] A.L. Pergament, P.P. Boriskov, A.A. Velichko, N.A. Kuldin, Switching effect and the metal–insulator transition in electric field, J. Phys. Chem. Solids 71 (2010) 849–874.
[5] H.T. Kim, B.G. Chae, D.H. Youn, S.L. Maeng, G. Kim, K.Y. Kang, Y.S. Lim, Mechanism and observation of Mott transition in VO_2-based two- and three-terminal devices, New J. Phys. 6 (2004) 1–19.
[6] C. Chen, Z. Zhou, Optical phonons assisted infrared absorption in VO_2 based bolometer, Appl. Phys. Lett. 91 (2007) 011107–011109.
[7] S. Saitzek, G. Guirleo, F. Guinneton, L. Sauques, S. Villain, K. Aguir, C. Leroux, J.R. Gavarri, New thermochromic bilayers for optical or electronic switching systems, Thin Solid Films 449 (2004) 166–172.
[8] D.P. Partlow, S.R. Gurkovich, K.C. Radford, L.J. Denes, Switchable vanadium oxide films by a sol–gel process, Appl. Phys. 70 (1991) 443–452.
[9] M. Soltani, M. Chaker, E. Haddad, R. Kruzelesky, 1 × 2 optical switch devices based on semiconductor-to-metallic phase transition characteristics of VO_2 smart coatings, Meas. Sci. Technol. 17 (2006) 1052–1056.
[10] B.J. Kim, Y.W. Lee, B.G. Chae, S.J. Yun, S.Y. Oh, H.T. Kim, Y.S. Lim, Temperature dependence of the first-order metal–insulator transition in VO_2 and programmable critical temperature sensor, Appl. Phys. Lett. 90 (2007) 023515–023517.
[11] H. Liu, A. Rua, O. Vasquez, V.S. Vikhnin, F.E. Fernandez, L.F. Fonseca, O. Resto, S.Z. Weisz, Optical and nonlinear optical response of light sensor thin films, Sensors 5 (2005) 185–198.
[12] S.M. Babulanam, T.S. Eriksson, G.A. Niklasson, C.G. Granqvist, Thermochromic VO_2 films for energy-efficient windows, Sol. Energ. Mater. 16 (1987) 347–363.
[13] T.D. Manning, I.P. Parkin, M.E. Pemble, M.E.D. Sheel, D. Vernardou, Intelligent window coatings: atmospheric pressure chemical vapor deposition of tungsten-doped vanadium dioxide, Chem. Mater. 16 (2004) 744–749.
[14] M.E. Spahr, P. Stoschitzkj-Bitterli, R. Nesper, O. Haas, J.P. Novak, Vanadium oxide nanotubes. A new nanostructured redox-active material for the electrochemical insertion of lithium, J. Eletrochem. Soc. 146 (1999) 2780–2783.
[15] C. Tsang, A. Manthiram, Synthesis of nanocrystalline VO_2 and its electrochemical behavior in lithium batteries, J. Electrochem. Soc. 144 (1997) 520–524.
[16] W. Li, J.R. Dahn, D.S. Wainwright, Rechargeable lithium batteries with aqueous electrolytes, Science 264 (1994) 1115–1118.
[17] S. Zhang, Y. Li, C. Wu, F. Zheng, Y. Xie, Novel flowerlike metastable vanadium dioxide (B) micronanostructures: facile synthesis and application in aqueous lithium ion batteries, J. Phys. Chem. C 113 (2009) 15058–15067.

[18] I. Stojković, N. Cvjetićanin, I. Pašti, M. Mitrić, S. Mentus, Electrochemical behaviour of V_2O_5 xerogel in aqueous $LiNO_3$ solution, Electrochem. Commun. 11 (2009) 1512–1514.

[19] I. Stojković, N. Cvjetićanin, S. Marković, M. Mitrić, S. Mentus, Electrochemical behaviour of V_2O_5 xerogel and V_2O_5 xerogel/C composite in an aqueous $LiNO_3$ and $Mg(NO_3)_2$ solutions, Acta Phys. Pol. A 117 (2010) 837–840.

[20] N. Cvjetićanin, I. Stojković, M. Mitrić, S. Mentus, Cyclic voltammetry of $LiCr_{0.15}Mn_{1.85}O_4$ in an aqueous $LiNO_3$ solution, J. Power Sources 174 (2007) 1117–1120.

[21] I. Stojković, N. Cvjetićanin, S. Mentus, The improvement of the Li-ion insertion behaviour of $Li_{1.05}Cr_{0.10}Mn_{1.85}O_4$ in an aqueous medium upon addition of vinylene carbonate, Electrochem. Commun. 12 (2010) 371–373.

[22] J. Liu, Q. Li, T. Wang, D. Yu, Y. Li, Metastable vanadium dioxide nanobelts: hydrothermal synthesis, electrical transport, and magnetic properties, Angew. Chem. Int. Ed. 43 (2004) 5048–5052.

[23] X. Chen, X. Wang, Z. Wang, J. Wan, J. Liu, Y. Qian, An ethylene glycol reduction approach to metastable VO_2 nanowire arrays, Nanotechnology 15 (2004) 1685–1687.

[24] G. Li, K. Chao, H. Peng, K. Chen, Z. Zhang, Low-valent vanadium oxide nanostructures with controlled crystal structures and morphologies, Inorg. Chem. 46 (2007) 5787–5790.

[25] J. Li, Z. Su, B. Yang, S. Cai, Z. Dong, J. Ma, R. Li, A facile and environmentally friendly chemical route for the synthesis of metastable VO_2 nanobelts, J. Phys. Chem. Solids 71 (2010) 407–411.

[26] F.J. Quites, H.O. Pastore, Hydrothermal synthesis of nanocrystalline VO_2 from poly(diallyldimethylammonium) chloride and V_2O_5, Mater. Res. Bull. 45 (2010) 892–896.

[27] G. Li, K. Chao, C. Zhang, Q. Zhang, H. Peng, K. Chen, Synthesis of urchin-like VO_2 nanostructures composed of radially aligned nanobelts and their disassembly, Inorg. Chem. 48 (3) (2009) 1112–1167.

[28] G.S. Zakharova, I. Hellmann, V.L. Volkov, Ch. Taschner, A. Bachmatiuk, A. Leonhardt, R. Klingeler, B. Buchner, Vanadium dioxide nanobelts: hydrothermal synthesis and magnetic properties, Mater. Res. Bull. 45 (2010) 1118–1121.

[29] C. Cao, Y. Gao, H. Luo, Pure single-crystal rutile vanadium dioxide powders: synthesis mechanism and phase-transformation property, J. Phys. Chem. C 112 (2008) 18810–18814.

[30] P. Pinceloup, C. Courtois, J. Vicens, A. Leriche, B. Thierry, Evidence of a dissolution–precipitation mechanism in hydrothermal synthesis of barium titanate powders, J. Eur. Ceram. Soc. 19 (1999) 973–977.

[31] Y. Zhang, X. Liu, G. Xie, L. Yu, S. Yi, M. Hu, C. Huang, Hydrothermal synthesis, characterization, formation mechanism and electrochemical properties of $V_3O_7{\cdot}H_2O$ single-crystal nanobelts, Mater. Sci. Eng. B 175 (2010) 164–171.

[32] W. Jiang, J. Ni, K. Yu, Z. Zhu, Hydrothermal synthesis and electrochemical characterization of VO_2 (B) with controlled crystal structures, Appl. Surf. Sci. 257 (2011) 3253–3258.

[33] G. Armstrong, J. Canales, A.R. Armstrong, P.G. Bruce, The synthesis and lithium intercalation electrochemistry of VO_2(B) ultra-thin nanowires, J. Power Sources 178 (2008) 723–728.

[34] H. Liu, Y. Wang, K. Wang, E. Hosono, H. Zhou, Design and synthesis of a novel nanothorn VO_2 (B) hollow microsphere and their application in lithium-ion batteries, J. Mater. Chem. 19 (2009) 2835–2840.